

## NONRECURSIVE FILTER TECHNIQUES IN DIGITAL PROCESSING OF REMOTE SENSING IMAGERY

M.Ehlers, E.Dennert-Möller, D.Kolouch and P.Lohmann  
Institute of Photogrammetry and Engineering Surveys  
University of Hannover  
Federal Republic of Germany  
Commission VII, WG VII/1

### ABSTRACT

At the present state nonrecursive filter techniques seem to be sufficient for a lot of tasks in the digital evaluation of remote sensing imagery. Recent experiences show that the choice of filter algorithms depends on evaluation goal, recording sensor, desired accuracy and computation time. Specific aims of image processing at the Institute for Photogrammetry of Hannover University are: geometric rectification by means of correlation techniques, thermal and thematic mapping of coastal and marine areas using multispectral scanner data and sea floor mapping with interferometric sidescan-sonar.

All pictures require previous filtering before the desired evaluation can be executed. Representative examples and the appropriate filter algorithms are presented. Results of image evaluation without filtering are compared to those after filtering. It can be proved that in some cases successful image processing is only possible with previous sensor-specific filtering.

### Introduction

Many tasks of digital evaluation of remote sensing imagery require image filtering, either as pre-processing or as post-processing for better visual interpretation. Numerous operations on the data can be interpreted as filtering (HAMMING 1977). Thus, when processing data, people are constantly filtering without knowing that they are doing so.

Common filter techniques like moving average for noise reduction or Sobel-filtering for edge detection are well-known and worldwide in use (PRATT 1978, CASTLEMAN 1979). But standard methods do not consider the evaluation target and/or the image information. On the other hand, very complex methods for image enhancement are proposed from electrical engineers with nonlinear and recursive approaches barely to understand for the 'normal' user in remote sensing. This paper tries to present image filtering procedures that are easier to design and to perform, but that are considering evaluation target and image content. In most cases linear techniques are discussed. If possible, a reduction from two to one dimension is performed for an easier filter design and understanding. All presented examples are processed at the digital image processing system MOBI-DIVAH of Hannover University (DENNERT-MÖLLER et al. 1982). Although the filter functions depend on image sensor and evaluation task we try to give a mutual basic approach for individual filter design, if possible.

### Fundamentals

#### Definitions

A **digital image** can be defined as discrete, integer two-dimensional signal  $s(n,m)$ ;  $n = 1, \dots, N$ ,  $m = 1, \dots, M$ .  $s$  is generated by equidistant sampling and quantization of

analog imagery (e.g. ground signal, photograph, map). A **two-dimensional [2D] filter** is a mapping  $F$  which maps an input image into an output image  $g$  without geometric transformation.

If  $g_1 = F\{s_1\}$  and  $g_2 = F\{s_2\}$  and

$$c \cdot g_1 + g_2 = F\{c \cdot s_1 + s_2\} \quad (1)$$

for an arbitrary constant  $c$ , then  $F$  is called **linear**. Furthermore, if

$$g(n-n_0, m-m_0) = F\{s(n-n_0, m-m_0)\} \quad (2)$$

for arbitrary integers  $n_0, m_0$ , then  $F$  is called **shift-invariant**. The unit sample  $u_0(n,m)$  is defined by

$$u_0(n,m) = \begin{cases} 1 & \text{for } n=m=0 \\ 0 & \text{otherwise} \end{cases}$$

$s(n,m)$  can be written as the summation of constants times the shifted unit sample:

$$s(n,m) = \sum_{k=-\infty}^{\infty} \sum_{l=-\infty}^{\infty} s(k,l) u_0(n-k, m-l) \quad (3)$$

So, if  $g(n,m) = F\{s(n,m)\}$  then

$$g(n,m) = \sum_{k=-\infty}^{\infty} \sum_{l=-\infty}^{\infty} s(k,l) F\{u_0(n-k, m-l)\}$$

The unit sample response,  $h(n,m)$ , of the system is defined by

$$h(n,m) = F\{u_0(n,m)\}.$$

Therefore

$$g(n,m) = \sum_{k=-\infty}^{\infty} \sum_{l=-\infty}^{\infty} s(k,l) h(n-k, m-l) \quad (4)$$

Thus the output signal  $g$  is the input convolved with the unit sample response of the filter. If  $h(n,m)$  is finite (or zero outside a finite area) then the filter is called **nonrecursive**.

### Filtering in the spatial and frequency domain

Linear filtering according to (4) can be performed in the spatial or frequency domain. It can be shown (HUANG 1975) that the complex functions  $e^{j\omega t}$  and  $e^{-j\omega t}$  are eigenfunctions for linear, shiftinvariant (LSI) systems:

$$F\{e^{j\omega t}\} = \lambda(\omega) e^{j\omega t}$$

with  $j = \sqrt{-1}$  and  $\omega = 2\pi f$ . This leads to the **Fourier transform** of signals. In case of a two-dimensional discrete signal  $s$  the Fourier transform  $S$  can be written as

$$S(u,v) = \frac{1}{N \cdot M} \sum_{n=0}^{N-1} \sum_{m=0}^{M-1} s(n,m) e^{-2\pi j \left[ \frac{u \cdot n}{N} + \frac{v \cdot m}{M} \right]} \quad (5)$$

with  $u,v$  and the frequency in  $x$ - and  $y$ -direction. Hence, filtering of an image can be

performed either in the spatial or frequency domain. The convolution with the unit sample response  $h$  according to (4) corresponds to a multiplication of  $S$  with the Fourier transform of  $h$  in the frequency domain. Fig.1 shows the relations between filtering in both regions.  $H$  is the Fourier transform of the unit sample response  $h$ , and  $*$  is used as abbreviation for the convolution integral.

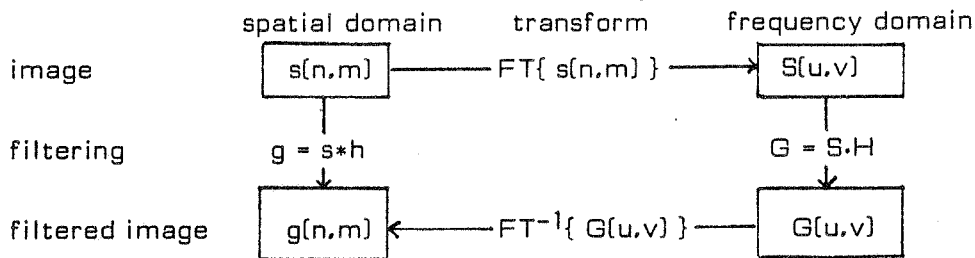


Fig.1: Filtering in the spatial and frequency domain

## Linear Filter Performance

### Spatial domain approach

As at the evaluation of remote sensing imagery spatial  $3 \times 3$  window LSI-operating techniques (e.g. moving average, Laplacian filters) are well-known and worldwide in use, they will not be discussed here. In the following we aim at the development and performance of LSI-filters, which are derived from sensor and task specific considerations. Wherever possible we try to execute a  $2D \rightarrow 1D$  reduction for raising computation speed and easier handling.

### Increase in correlation probability

Multisensoral evaluation of remote sensing imagery (e.g. classification or change detection) requires the knowledge of identical points in different images of the same area. The geometric transformations between these 'control points' allow the estimation of rectification parameters. The identification of these control points can be achieved by applying digital correlation techniques (EHLERS 1984). One great problem - especially in images with low signal-to-noise ratio - is the failure of the correlation function. Tidal land imagery of the German North Sea coast contains very homogeneous structure. Fig.2 shows 4 corresponding sectors of two overlapping frame camera photographs from tidal lands with their according power spectra. The aerial photography was digitized with a sampling rate of  $100 \mu\text{m}$ .

In one image, the reference image, four  $11 \times 11$  windows are chosen as pattern matrices for the correlation process (fig.3). In the second image, the whole corresponding  $128 \times 128$  pixel sections serve as search matrices. Two different objective functions for the correlation process were applied:

- the normal product moment correlation coefficient
- the intensity correlation coefficient derived from coherent optical considerations (EHLERS 1982).

The results are presented in fig.4 showing the maxima of function a) (white) and of function b) (black, if different). Even in photogrammetric unitemporal images, both correlation functions show possibility of error.

Picture preprocessing is required to achieve better results.

A low pass filter according to the power spectra of the image sections was designed, which considers 95 % of the signal information. The filter transfer function in the frequency domain was chosen as one-dimensional curve (fig.5). The frequency axis is normalized with respect to the sampling frequency.

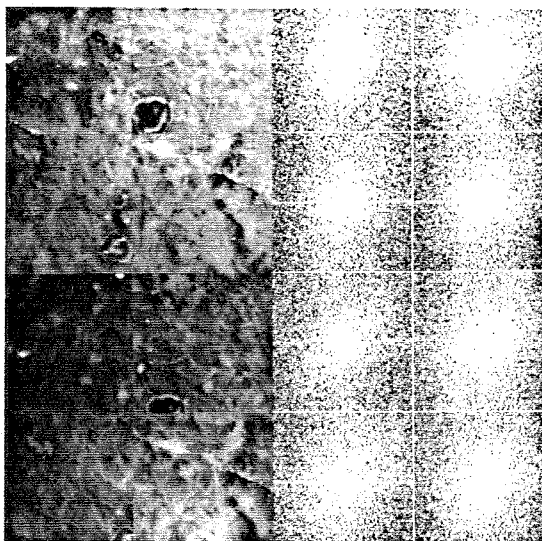


Fig.2: Aerial photography sections with their according power spectra

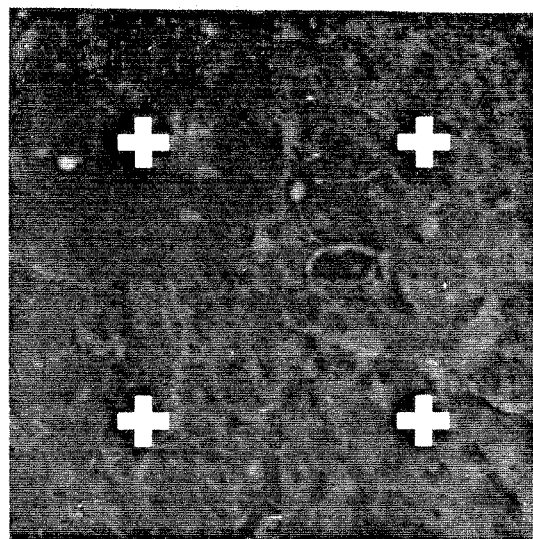


Fig.3: Reference image with correlation points

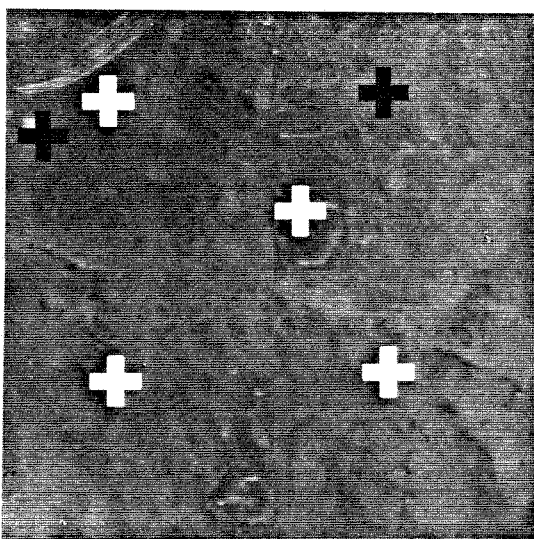


Fig.4: Search image with correlation maxima (white = function a), black = function b), if different)

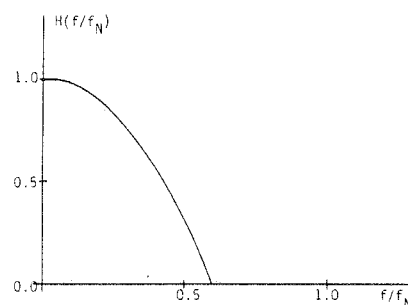


Fig.5: Filter transfer function

The filter transfer function was made two-dimensional by rotation, and transformed into a filter matrix by inverse Fourier transformation. In this way isotropic 2D filter matrices can be designed by 1D estimation. The effects of filtering with the resulting 9x9 matrix on the correlation probability can be seen in fig.6. Human eye control verifies that both objective functions indicate the correct values for the position of the control points. No other of several additionally tested filters (band pass, high pass or median) was error-free (EHLERS 1982).

Low pass filtering, designed from spectral image analysis, increases the SNR and the correlation probability. Pre-processing for this purpose necessitates image-specific knowledge (here spectral knowledge) to improve the quality of automatic mapping processes.

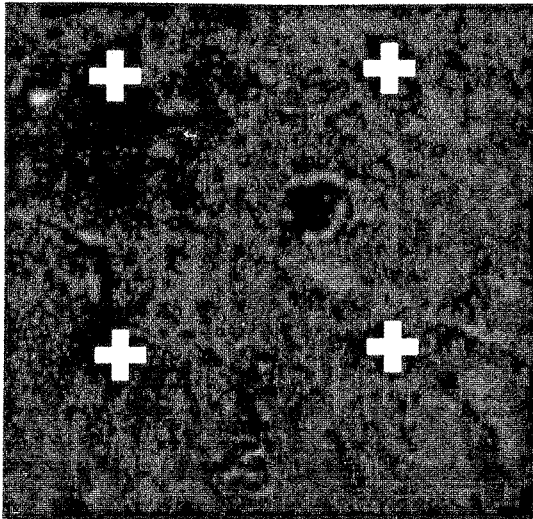


Fig.6: Filtered search image with correlation maxima

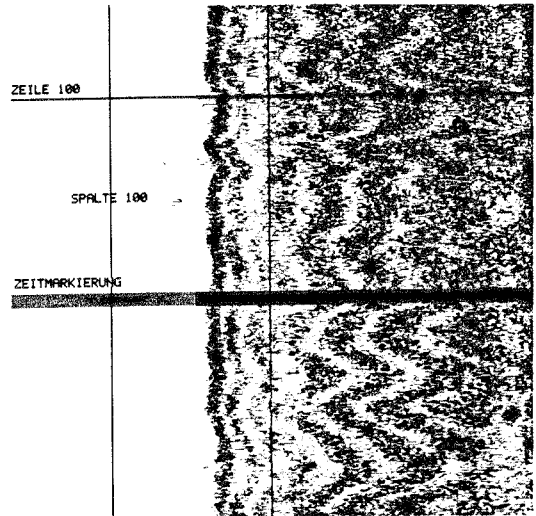


Fig.7: Interferometric Side-Scan-SONAR image (ISSS)



Fig.8: ISSS image line

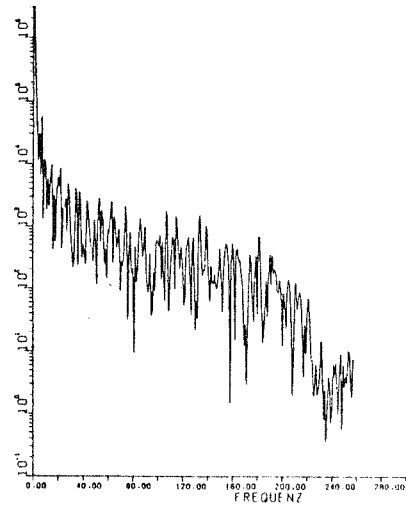


Fig.9: Power spectrum of ISSS image line

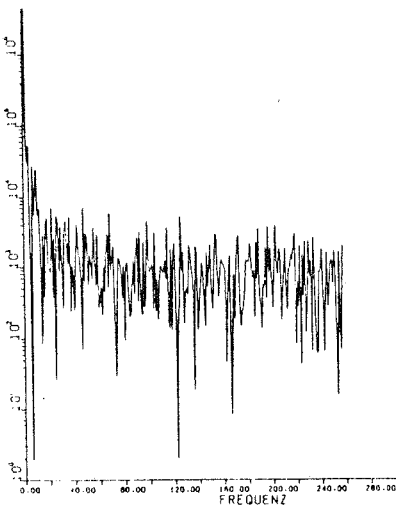


Fig.10: Power spectrum of ISSS image column

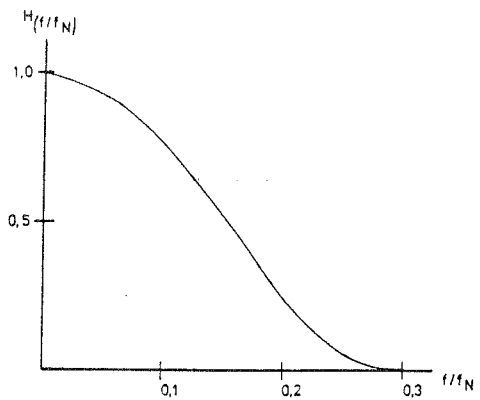


Fig.11: Filter transfer function

## Fringe pattern extraction in SONAR imagery

Another application of two-dimensional filter design is given in imagery of an active sensor for sea floor mapping, the interferometric Side-Scan-SONAR-system (ISSS). The artificially generated Lloyd-Mirror effects create fringe pattern in the ISSS imagery which allows the determination of water depth (KOLOUCH 1983).

A great problem for automatic detection of maxima and minima in the ISSS fringe pattern is the high noise level in the ISSS images (fig.7). Fig.8 shows one line of the image marked in fig.7. Common noise reduction techniques like moving average or median filtering are not sufficient (EHLERS and KOLOUCH 1982). With a spectral analysis image specific filters can be derived. Fig.9 shows the logarithmic power spectrum of the image line presented in fig.8. To estimate the pure noise part, the power spectrum of a column in an image section with almost no interferometric information was computed (fig.10). The column is also marked in fig.7. The line power spectrum shows a strong intensity decrease with increasing frequency, whereas the column power spectrum contains no significant loss of intensity beyond a frequency of  $f_g \sim 0.2 f_s$  ( $f_s$  = sampling frequency)

A one-dimensional low pass filter transfer function is designed to remove spectral information beyond  $f_g$  (fig.11). With the above specified technique, the one-dimensional filter function is transformed into a 11x11 two-dimensional filter matrix. The results of ISSS filtering are presented in fig.12 and 13. Fig.12 shows the same line as fig.7. The low pass filtered image allows an automatic maximum estimation in the ISSS imagery (EHLERS and KOLOUCH 1982).

## Frequency domain approach

Another way of LSI filtering is the direct multiplication of the image spectrum with a given filter transfer function. This way contains two main advantages: it is faster beyond a certain size of a filter matrix, and anisotropic filtering can be easily performed. One great disadvantage, caused by the discrete technique of Fourier transform, is the 'Gibb's phenomenon' (HAMMING, 1977). To avoid distortions in the spatial domain, filter design in the frequency domain has to be performed with great care. The MOBI-DIVAH image processing system allows filter smoothing with Gaussian, sinc- or interactively designed functions (PIECHEL 1983).

## Direction dependent filtering

The frequency approach allows the direct amplification or suppression of direction dependent information. Fig.14-16 show an example on an artificial test pattern (fig.14). Fig.15 represents the filter design in the frequency domain with a main amplification angle of 45°. Fig.16 shows the filtered image with the remaining information right-angled to the frequency amplification. With the direct frequency approach desired edge or fringe pattern direction can be extracted. Fig.17 shows another ISSS imagery which is to be filtered with 90° and 45° emphasis. The designed filter functions can be found in fig.18 and 19. Fig.20 and 21 show the direction dependent filter results. Combined with subsequent low pass filtering this technique seems to be an effective tool for extraction of pattern directions.

## Correction of light fall-off in photographic imagery

One great disadvantage at the evaluation of photographic imagery - especially of those taken by superwide-angled camera lenses - is the light fall-off from the principal point to the image edges (MICHAELIS et al. 1984).

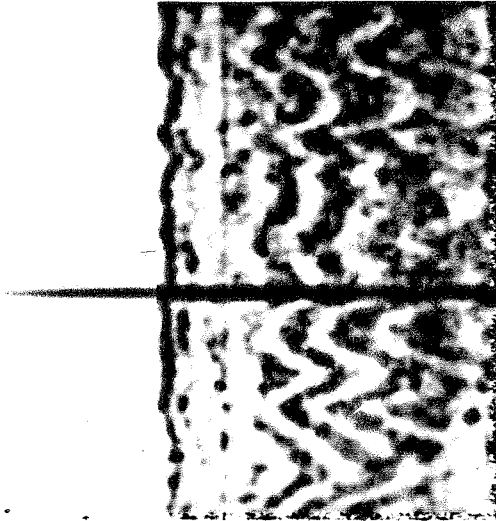


Fig.12: Filtered ISSS image



Fig.13: Filtered ISSS image line

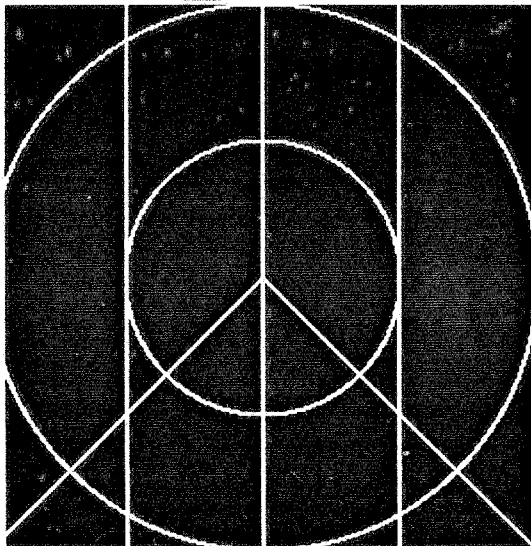


Fig.14: Test pattern

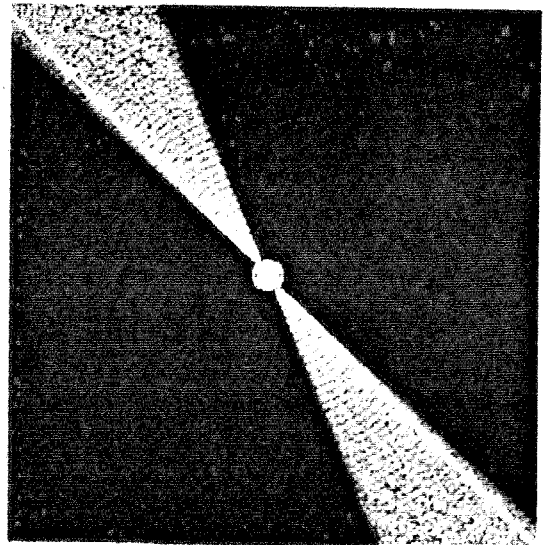


Fig.15: Filter design in the frequency domain

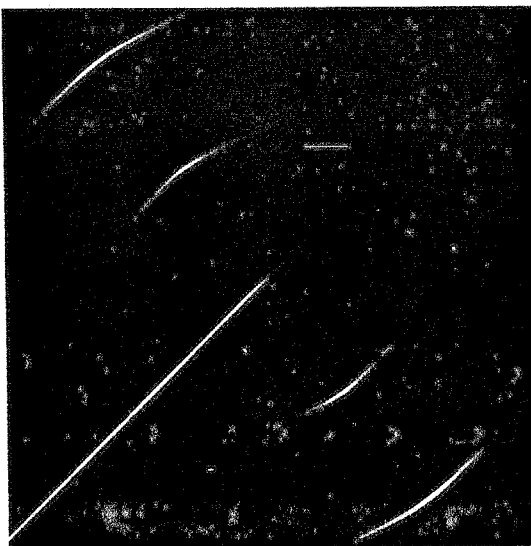


Fig.16: Filtered test pattern

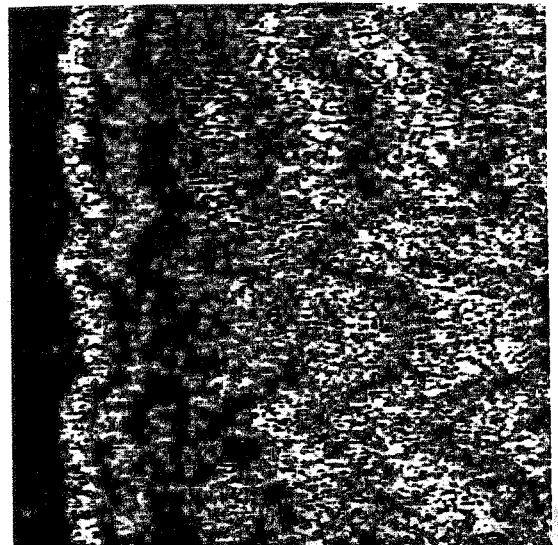


Fig.17: ISSS image

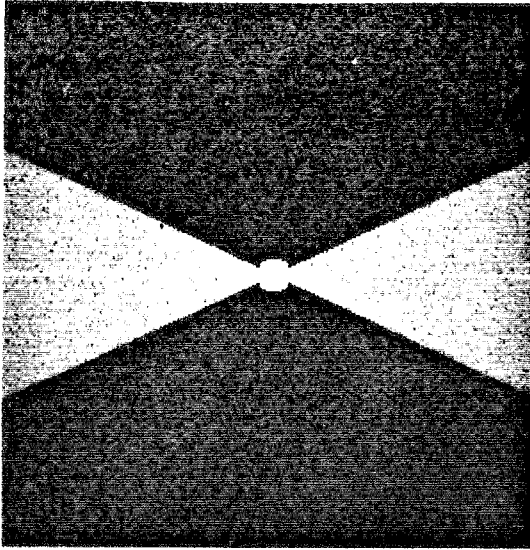


Fig.18: Frequency domain filter design (90°)

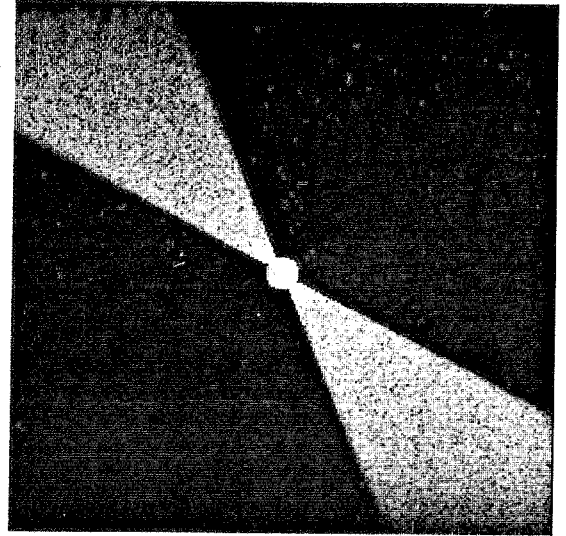


Fig.19: Frequency domain filter design (45°)

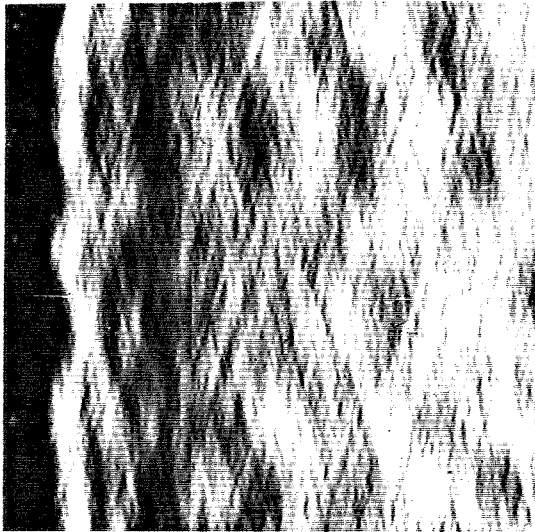


Fig.20: Filtered ISSS image (90° enhanced)

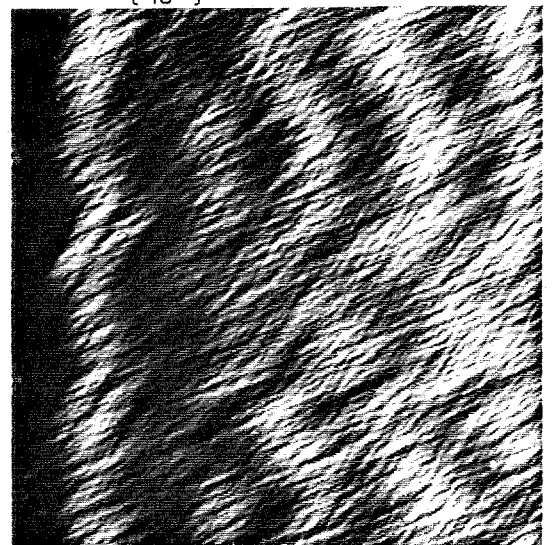


Fig.21: Filtered ISSS image (45° enhanced)



Fig.22: Frame camera image (flying altitude 11 km)

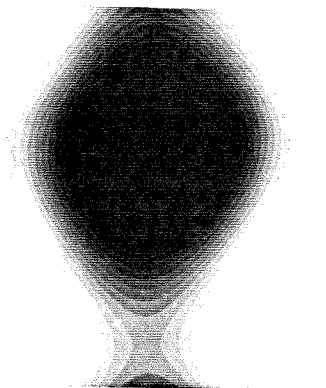


Fig.23: Light fall-off

Although sometimes almost invisible for the human eye (or automatically analog filtered and interpreted) the light fall-off leads to severe errors in multispectral classification (DENNERT-MÖLLER and EHLERS 1982). In theory, the light fall-off is radially



symmetric, but in practice it depends on sun position, illumination angle, and recording and environmental conditions (MICHAELIS et al. 1984). Fig.22 shows a contrast-enhanced frame camera image of the North Sea coast taken with a superwide-angled camera lens. The light fall-off can be extracted by an extreme low pass filter, because it should be located at 1 cycle/image in the frequency domain. Its estimation from frequency domain filtering is shown in fig.23 (for better visual interpretation, a positive-negative change has been executed). The corrected image is presented in fig.24.

### Nonlinear filter performance

As there is no practically useful general theory of nonlinear operations, we have to treat each nonlinear filter procedure individually as it comes up in particular applications (HUANG 1975). We will refer to only two different types of nonlinear operations associated with specific evaluation problems.

#### Sorting procedures

A special class of nonlinear filters easy to be designed are those that do not create new image grey values but put them into a new order. A very important edge-preserving sorting filter is the median filter, replacing the filtered element by the median value of its environment. Median filters have been found effective in reducing certain types of noise and periodic interference patterns without severely degrading the signal (HUANG 1981). The theoretic behaviour of median filters is very difficult, so that only few results exist. In general, it can be ascertained, that median filtering is a nonlinear shift varying low pass filter with 'fixed points' where the signal remains unchanged. Fig.25 underlines this statement. It shows a (one-dimensional) sample with its moving median filtered output of size 3 and 5. The output is identical to the input (5-sample median) or a shifted replica of the input (3-sample median).

Also, if a sample is monotoneous, median filtering leaves the signal unchanged. The edge preservation of median filtering is shown in fig.26 showing an edge plus noise sequence filtered with median and moving average operations.

High efficiency median filtering shows in density sliced or classified images. The procedure 'cleans' the output image for better visual interpretation or map printing. Fig.27 presents an unfiltered classified LANDSAT image of the North Sea coast, fig.28 the 5x5 median filtered output. Fig.29 shows the filtered output image if the median value is replaced by the most frequent environmental value, the mode value. Although the results look very similar, the latter filter seems to be more appropriate for classified imagery.

#### Scanner-regression-filter (SRF)

For mapping of sewage from power stations thermal infrared information can be used. Thermal scanner imagery is often disturbed by 'scan-line-noise', especially over homogeneous areas like water surface. Fig.30 shows the thermal channel of a Bendix M2S-Scanner scene recorded at a flying altitude of 1600 m. Neither common spatial or frequency domain filter techniques are sufficient to reduce the scan-line-noise in a desired manner necessary to achieve highly accurate temperature mapping (EHLERS and LOHMANN 1982).

For the design of a filter, which is only valid for scan-line-noise one can consider that this noise  $n$  is additive and column independent. Thus the disturbed signal  $g$  can be written

$$g(x,y) = g_0(x,y) + n(x)$$



Fig.24: Corrected image

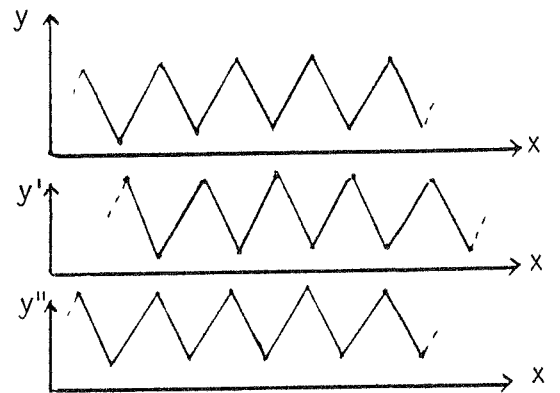


Fig.25: Original sample  $y$ , moving median filtered  $y'$  (size 3), moving median filtered  $y''$  (size 5)

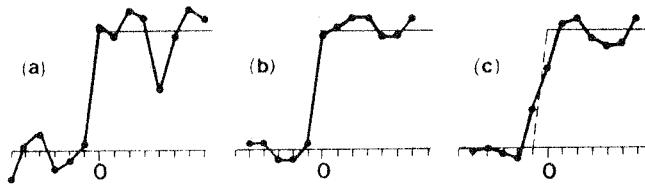


Fig.26: Edge plus noise sequence (a) after median filtering (b), after moving average filtering (c)



Fig.27: Classified LANDSAT image



Fig.28: 5x5 median filtered image



Fig.29: 5x5 mode filtered image



Fig.30: Thermal image (unfiltered)

with  $g_0$  the original ground signal. With this assumption the noise can be estimated in a relative homogeneous image area (EHLERS 1983). Fig.31 shows the window for the used SNR estimation. The SNR is computed as difference between the actual mean values of the image lines and their linear regression model

$$\text{SRF}(x) = a_1 + a_2x - \int_{y_0}^{y_0} g(x,y)dy$$

$a_1$  and  $a_2$  are computed using least square techniques. Then the SRF is added to the entire image. The filtered image is shown in fig.32. Better visual control of SRF filtering shows the comparison of isothermal presentation without filtering, after filtering with moving average and SRF (fig.33-35). The temperature accuracies are raised from 0.5 K up to 0.2 K (EHLERS and LOHMANN 1982).

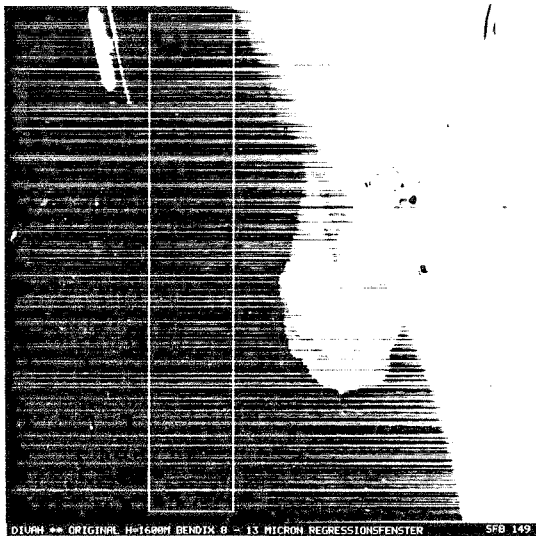


Fig.31: Window design for SRF estimation



Fig.32: SRF filtered image

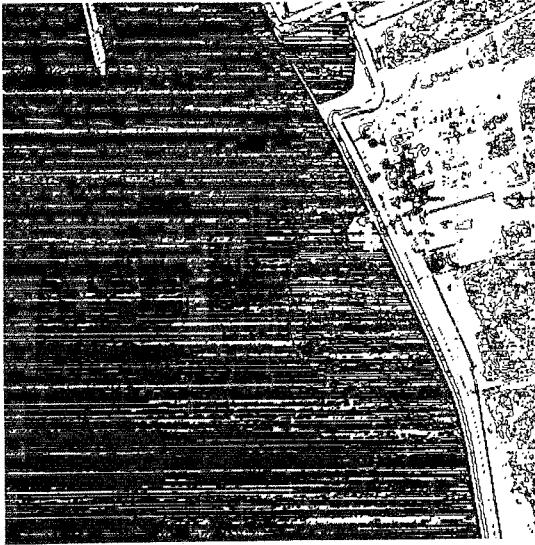


Fig.33: Isothermals/original image

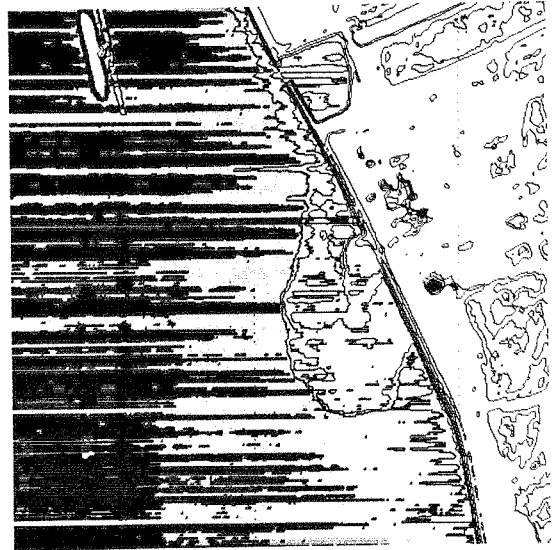


Fig.34: Isothermals/moving average

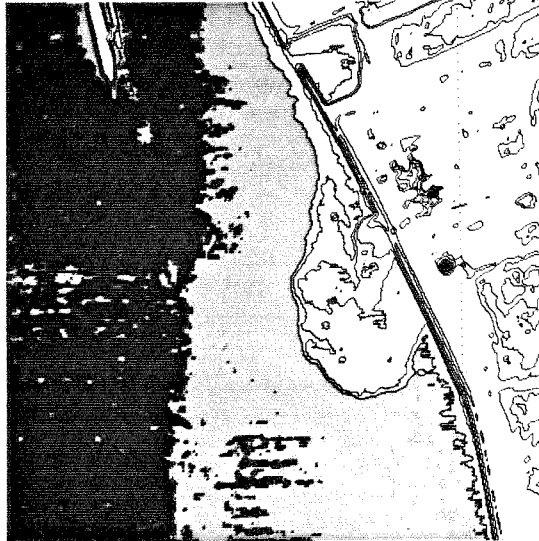


Fig.35: Isothermals/SRF

### Conclusions

The paper demonstrates with typical examples at the digital processing of remote sensing imagery that almost all evaluation targets need precedent image filtering. These filter procedures have to be associated with a certain sensor (e.g. thermal scanner or SONAR imagery) or a certain task (e.g. thematic mapping or image correlation). In some cases image preprocessing is the only way to provide useful results. It can be shown that nonrecursive and linear-shift-invariant filtering or simple nonlinear operations are sufficient for various aims. Sometimes they are even superior to highly sophisticated methods. So digital filtering in the MOBI-DIVAH image processing system follows the rule "If an elementary filter has sufficient results, we are not interested in always finding the best method in designing very complex filters (HAMMING 1977)."

## References

- CASTLEMAN, K. (1979): Digital Image Processing, Prentice-Hall, 429 p.
- DENNERT-MÖLLER, E. and M.EHLERS (1982): Auswertung von Reihenmeßkammer- und FLugzeugabtasteraufnahmen aus Wattgebieten, Bildmessung und Luftbildwesen 50, pp.59-67.
- DENNERT-MÖLLER, E., M.EHLERS, D.KOLOUCH, and P.LOHMANN (1982): Das digitale Bildverarbeitungssystem MOBI-DIVAH, Bildmessung und Luftbildwesen 50, pp.201-203.
- EHLERS, M. (1982): Increase in Correlation Accuracy of Remote Sensing Imagery by Digital Filtering, Photogrammetric Engineering and Remote Sensing, Vol. 48, pp.415-420.
- EHLERS, M. (1983): Fast Two-Dimensional Filtering of Thermal Scanner Data with One-Dimensional Estimation, Proc. of the XVIIth Int.Symp. on Rem.Sens. of Environment, Ann Arbor, USA, May 9-13.
- EHLERS, M. (1984): The Automatic DSCOR System for Rectification of Space-Borne Imagery as Basis for Map Production, Pres.Paper, XVth Int.Congress of ISPRS, Rio de Janeiro, Brasil, June 17-29.
- EHLERS, M. and D.KOLOUCH (1982): Interferometrisches Side-Scan Sonar. Datengewinnung und digitale Filterung, Bildmessung und Luftbildwesen 50, pp.207-210.
- EHLERS, M. and P.LOHMANN (1982): Digital Enhancement of Noisy Scanner Imagery, Proc.of the Int.Symp. Comm VII-ISPRS, Toulouse, pp.135-143.
- HAMMING, R.W. (1977): Digital Filters, Prentice-Hall, New Jersey, 226 p.
- HUANG, T.S. (ed.) (1975): Picture Processing and Digital Filtering, Springer, Berlin, Heidelberg, New York, 289 p.
- HUANG, T.S. (ed.) (1981): Two-Dimensional Digital Signal Processing II. Transforms and Median Filters, Springer, Berlin, Heidelberg, New York, 222 p.
- KOLOUCH, D. (1983): Interferometrisches seitwärts schauendes Sonar, Zeitschrift für Vermessungswesen, 108, pp.461-471.
- MICHAELIS, M., E.DENNERT-MÖLLER and M.EHLERS (1984): Correction of Light-Fall-Off in Photography by Means of Digital Statistical Methods, Pres.Paper, XVth Int.Congress of ISPRS, Rio de Janeiro, Brasil, June 17-29.
- PIECHEL, J. (1983): Erstellung und Erprobung eines Programms zur digitalen Filterung im Frequenzraum, Diploma thesis (unpublished), Universität Hannover
- PRATT, W.K. (1978): Digital Image Processing, J.Wiley & Sons, 750 p.